Disponible en **www.hormigonyacero.com**
Hormigón y Acero 2023; 74(299-300):187-198
https://doi.org/10.33586/hya.2022.3092

Compressive Behaviour of Steel-Fibre Reinforced Concrete in Annex L of New Eurocode 2

Comportamiento en compresión del hormigón reforzado con fibras de acero según el Anejo L del nuevo Eurocódigo 2

Gonzalo Ruiz[*, a], Ángel de la Rosa[a], Elisa Poveda[a], Riccardo Zanon[b], Markus Schäfer[b], & Sébastien Wolf[c]

[a] *ETS de Ingenieros de Caminos, C. y P., Universidad de Castilla-La Mancha, Avda. Camilo José Cela s/n, 13071 Ciudad Real, Spain*
[b] *Department of Engineering, University of Luxembourg, 6 rue Richard Coudenhove-Kalergi, L-1359 Luxembourg*
[c] *ArcelorMittal Fibres, Route de Finsterthal, L-7769 Bissen, Luxembourg*

Recibido el 15 de julio de 2022, aceptado el 8 de diciembre de 2022

ABSTRACT

This paper describes the model for the compressive stress-strain behaviour of steel-fibre reinforced concrete (SFRC) in Annex L of the new Eurocode 2 (CEN, Eurocode 2: Design of concrete structures. Part 1-1: General rules – Rules for buildings, bridges and civil structures, prEN 1992-1-1: 2022; EC2 in short), developed within CEN TC250/SC2/WG1/TG2 – Fiber reinforced concrete. The model uses functions obtained from correlations with an extensive database comprised of 197 welldocumented SFRC compressive tests and 484 flexural tests. We detailedly explain the model and derive the strain values for the parabola-rectangle model for ULS of SFRC in Annex L. In addition, we also use the model and the correlations with the database to provide a link between the compressive and the flexural performance classes in EC2, which allows a complete definition of any particular SFRC. Likewise, we derive parabola-rectangle strain values for each flexural performance class, which is mainly advantageous for the stronger flexural performance classes. Finally, we give an example showing the enhancement in strength and ductility of a composite steel-SFRC section endorsed with the new model, which results of 15% and 100%, respectively.

KEYWORDS: Compressive model for SFRC in Annex L of Eurocode 2, combined compression/flexural classification for any SFRC, relevant strains for ULS calculation, impact of the ductility and toughness enhancement of composite steel-SFRC sections on Eurocode 4.

RESUMEN

Este artículo describe la nueva ley tensión-deformación en compresión para hormigón reforzado con fibras de acero (HRFA) que propone el Anejo L del nuevo Eurocódigo 2 (CEN, Eurocódigo 2: Diseño de estructuras de hormigón. Parte 1-1: Reglas generales – Reglas para edificios, puentes y estructuras civiles, prEN 1992-1-1: 2022; en breve, EC2), desarrollado dentro del grupo de trabajo CEN TC250/SC2/WG1/TG2 – Hormigón reforzado con fibras. La nueva ley utiliza funciones obtenidas a través de correlaciones con una extensa base de datos compuesta por ensayos de HRFA bien documentados, 197 a compresión y 484 a flexión. En el artículo explicamos detalladamente la nueva ley, y deducimos los nuevos valores de deformación para la ley parábola-rectánculo en ELU para HRFA en el Anejo L. Además, también usamos la nueva ley y las correlaciones con la base de datos para vincular las clases de compresión y flexión del EC2, lo cual permite una definición completa de cualquier HRFA. Del mismo modo, deducimos nuevos valores de deformación para la ley parábola-rectánculo en ELU para cada clase de flexión, que añaden ductilidad a las clases de flexión más resistentes. Finalmente, incluimos un ejemplo que muestra la mejora en resistencia y ductilidad de una sección mixta de acero-HRFA calculada con la nueva

>>

* Persona de contacto / *Corresponding author*:
Correo-e / *e-mail*: Gonzalo.Ruiz@uclm.es (Gonzalo Ruiz).

How to cite this article: Ruiz, G., De La Rosa, Á., Poveda, E., Zanon, R. Schäfer, M., & Wolf, S. (2023) Compressive Behaviour of Steel-Fibre Reinforced Concrete in Annex L of New Eurocode 2, *Hormigón y Acero*, 74(299-300):187-198 https://doi.org/10.33586/hya.2022.3092

ley, que resulta ser un 15% más resistente y un 100% más dúctil que la misma sección con hormigón sin fibras de la misma clase de compresión.

PALABRAS CLAVE: Ley tensión-deformación en compresión para HRFA en el Anejo L del Eurocódigo 2, clasificación combinada compresión/flexión para cualquier HRFA, deformaciones relevantes para el cálculo de ELU, repercusión en la mejora de la ductilidad y tenacidad de secciones mixtas acero-HRFA en el Eurocódigo 4.

1
INTRODUCTION

The superior ductility and toughness provided by steel-fibre reinforcement to flexural elements are well known, mainly due to the higher residual flexural tensile strength after cracking [1–6]. This is achieved because steel fibres give the capacity to the concrete to overtake tension, and this capacity is increased in correlation with the fibres' type, the steel wire tensile strength, and the dosage rate of steel fibres in the concrete mix. This enables the use of steel-fibre reinforced concrete (SFRC) in many structural applications [1, 3, 7–9], mainly when controlling the cracking processes is a must [1, 10], like in tunnel lining segments [1, 11–20], industrial floors [1, 21, 22], elevated slabs, bearing rafts on ground, and on piles [23, 24], precast pipes [25] and others. This is why SFRC is included in several structural concrete design codes and regulations [26–35], although they only consider the response to tension and its influence on bending.

It is also known that increasing the compression strength of the concrete involves an increase in the flexural strength, and in turn, the addition of steel fibres increases the capacity of deformation and ductility when the maximum flexural load is exceeded [36]. There is much research that analyzes the flexural behaviour of SFRC in terms of tension, deformation and crack mouth opening displacement using relationships that take into account the characteristics associated with the reinforcement of the fibre [1, 2, 6, 37–47], principally the dosage rate, slenderness, and steel wire tensile strength.

On the other hand, the ductility and toughness increase after the maximum load of SFRC in compression has been thoroughly reported [48–64], and there are several compressive stress-strain models developed so far [50, 52, 54, 57, 58, 64–69]. Regrettably, most of them were calibrated with limited data, and their predictions failed when checked against other experimental sources, as pointed out by Bencardino *et al.* [70]. However, they reported that the model of Barros *et al.* [57] is very accurate. Indeed, it gave good results when used by Yoo *et al.* [36] to model the flexural and compressive strengths of concrete reinforced with amorphous steel fibres.

Disregarding the effective contribution of the fibres in compression when designing structural elements may lead to a waste of the capabilities of the material. For instance, additional ductility and toughness in compression may facilitate that steel elements in composite sections can work at their limits [71, 72]. Besides, as flexural and compressive behaviours of SFRC are interconnected, it follows that proper classification of SFRC requires establishing a link between the compression and flexural strength classes, which is not done in the current normative [26, 27]. All the above considered, Task Group CEN TC250/SC2/WG1/TG2, responsible for the new Annex L on SFRC, decided to study the compressive capacities of the material and draft a model that could account for them in a technological fashion. The outcome is the model in the draft of Annex L of the new Eurocode 2 [73] (EC2 in short). It is based on functions obtained from correlations with an extensive database comprised of 197 well-documented SFRC compressive tests and 484 flexural tests [1, 56, 57, 61, 62, 70, 74–88]. Detailed derivations of these functions are reported in [89–91].

The following section succinctly describes the stress-strain model as it appears in Annex L of EC2 [73]. For the sake of consistency, along with brevity in the description, the new model is based on the σ_c-ϵ_c equation for plain concrete proposed by Sargin [92] and implemented in Formula 5.6 of Section 5.1.6 (3) of EC2 [73]. The new model just changes the expressions for some of the coefficients in Formula 5.6 to account for the increased toughness and ductility of SFRC due to fibres. Subsequently, we comprehensively explain the model in a closed form and justify the strain values given for ULS calculations (Section 3). In Section 4 we provide a discussion based on the link between compressive and flexural classification (Subsection 4.1), the ductility in compression including the strain values defining the new expressions for each flexural performance class (4.2), and the impact of SFRC ductility on composite beams designed in accordance to Eurocode 4 [93] (4.3). Finally, we draw some conclusions in Section 5.

2
COMPRESSIVE BEHAVIOUR OF SFCR IN ANNEX L

2.1. Stress-strain relationship in compression for non-linear structural analysis of SFRC

The stress-strain relation for non-linear structural analysis of SFRC in Annex L of the new EC2 (version of November 10, 2022) [73], section L.5.5.2 (2), reads as follows:

"The relation between σ_c and ϵ_c in compression in Formula (5.6) may be used to model the response of SFRC to short-term uniaxial compression provided the following modifications in the parameters are made:

$$\epsilon_{c1}\,(‰) = 0.7\, f_{cm}^{1/3}\, (1 + 0.03\, f_{R,1k}) \tag{1}$$

and, for $\epsilon_{c1} < \epsilon_c \le \epsilon_{cu1}$:

$$k = 1 + \frac{20}{\sqrt{82 - 2.2\, f_{R,1k}}} \quad \text{and } \epsilon_{cu1} = k\, \epsilon_{c1}\text{''} \tag{2}$$

where f_{cm} and $f_{R,1k}$ must be inserted in MPa in Eqs. 1 and 2.

2.2. Stress distribution for SFRC in compression in ULS

Annex L also allows accounting for the superior toughness and ductility of SFRC in ULS —as compared to plain concrete— by enlarging the strain parameters that define the stress distribution. This is done in Section L.8.1 (4), which reads as follows:

> "The stress distribution according to Formula (8.4) may be modified for SFRC by applying ϵ_{c2} = 0.0025 and ϵ_{cu} = 0.006."

These parameters are 0.0020 and 0.0035, respectively, for concrete without fibres.

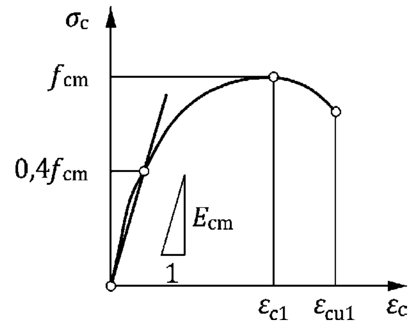

Figure 1. Stress-strain relation for plain concrete in compression (Figure 5.1, EC2 [73]).

3. EXPLANATION AND JUSTIFICATION OF THE COMPRESSIVE STRESS-STRAIN MODEL FOR SFRC IN ANNEX L

3.1. Stress-strain relationship in compression

The new σ_c-ϵ_c relationship for SFRC is built on the compressive model for plain concrete proposed by Sargin [92] and implemented in EC2 [73], Formula 5.6, that is:

$$\frac{\sigma_c}{f_{cm}} = \frac{k\eta - \eta^2}{1+(k-2)\eta} \tag{3}$$

where f_{cm} is the mean compressive strength (given in Table 5.1 of EC2 [73]); k is a parameter enforcing that the secant elastic modulus of the curve is E_{cm}, and is given by:

$$k = 1.05\ \epsilon_{c1} \frac{E_{cm}}{f_{cm}} \tag{4}$$

where ϵ_{c1} is the compressive strain corresponding to the concrete strength, i.e. the peak of the curve, and is obtained as:

$$\epsilon_{c1}\,[‰] = 0.7\, f_{cm}^{1/3} \leq 2.8‰ \tag{5}$$

Equation 5 needs that f_{cm} is in MPa. Note that k in Eq. 4 is non-dimensional whatever the system of units is used, but it would need that E_{cm} is in GPa and f_{cm} in MPa in case ϵ_{c1} is given in per mill as per Eq. 5.

Variable η of Eq. 3 is the ratio between the compressive strain, ϵ_c, and the compressive strain at the peak, ϵ_{c1}:

$$\eta = \frac{\epsilon_c}{\epsilon_{c1}} \tag{6}$$

where ϵ_c has the following limit value:

$$\epsilon_c < \epsilon_{cu1}\,[‰] = 2.8 + 14\,(1 - f_{cm}/108)^4 \leq 3.5‰ \tag{7}$$

which requires that f_{cm} is in MPa. Having the above definitions into account, Eq. 3 describes a non-dimensional stress-strain curve whose abscissa and ordinate are η and σ_c/f_{cm}, respectively. The dimensional stress-strain curve for plain concrete given by Eq. 3 is shown in Figure 1.

The new stress-strain relation for SFRC uses Eq. 3 but modifies the values of some of the parameters to account for the additional toughness and ductility provided by the steel fibres. The SFRC model keeps the values for f_{cm} and E_{cm} of the base concrete since it is proven that fibres have little influence on them [89– 91]. However, the strain for the peak of the curve, ϵ_{c1}, is increased as expressed in Eq. 1. The unit increase of the strain for the maximum stress is $0.03 f_{R,1k}$ ($f_{R,1k}$ in MPa), as disclosed in [91]. The rest of the curve parameters in Eq. 3 remain the same for the ramp-up part of the stress-strain curve, that is for $\epsilon_c \leq \epsilon_{c1}$ (or $\eta \leq 1$).

The downward stretch of the curve after ϵ_{c1} can also be represented using Eq. 3 provided a new value for the parameter k is taken, as expressed in Eq. 2. Note that with this new value for k the stress-strain curve has a maximum at $\epsilon_c = \epsilon_{c1}$ (η = 1), and intercepts the abscissa at $\epsilon_c = \epsilon_{cu1}$, where $\epsilon_{cu1} = k\,\epsilon_{c1}$ ($\eta_u = k$). So, the new value for k in Eq. 2 represents the increase in the critical strain relative to ϵ_{c1} [89, 91].

It bears emphasis that parameter k takes the following values for the two stretches —ascending and descending branches— of the stress-strain curve:

$$k = \begin{cases} 1.05\ \epsilon_{c1} \dfrac{E_{cm}}{f_{cm}} & \text{for} \quad \epsilon_c \leq \epsilon_{c1} \\ 1 + \dfrac{20}{\sqrt{82 - 2.2\, f_{R,1k}}} \quad (f_{R,1k}\ \text{in MPa}) & \text{for} \quad \epsilon_{c1} < \epsilon_c \leq \epsilon_{cu1} \end{cases} \tag{8}$$

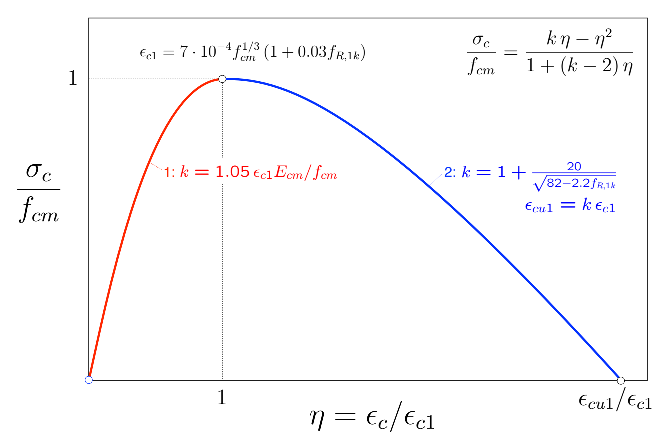

Figure 2. Non-dimensional stress-strain relationship for SFRC.

The new stress-strain curve for SFRC is plotted in Figure 2. Note that Figure 2 includes the equations and variables to be applied for building the complete compressive stress-strain model for SFRC.

The database we used for the multivariate analysis and subsequent model derivation contains results of SFRC with hooked-end fibres only. Thus, the equations derived in papers [89–91] are valid for this type of SFRC. However, the compressive σ-ϵ curve in Annex L is a function of $f_{R,1k}$ only (see Eqs. 1 and 2), which is a parameter that depends mainly on the compressive strength of the base concrete and the interface properties of the fibre [90], and very little on the hooks at the ends or the shape of the fibre. Therefore, the new compressive model can be used for SFRC reinforced with any type of steel fibre.

Previous versions of this stress-strain curve did not use Eq. 3 for the descending stretch, but an inverted parabola with the maximum in the peak of the compressive strength [89–91], which expression is:

$$\frac{\sigma_c}{f_{cm}} = 1 - \frac{1}{4}\,(\eta-1)^2\left(1-\frac{\sigma_R}{f_{cm}}\right) \tag{9}$$

where σ_R was called the residual compressive strength and is the value that the stress takes for $\eta = 3$. It was defined so because there was not a single stress-strain curve in the database that did not reach at least a final strain three times larger than the strain at the peak, which served to define a reference point to obtain the energy per unit volume absorbed in the database tests, which were called W_{c1} from 0 to ϵ_{c1}, and W_{c2} from ϵ_{c1} to 3 ϵ_{c1}. Besides, it seemed reasonable to define a *residual* compressive strength since it was analogous to the *residual* flexural strengths, $f_{R,i}$, which are accepted as relevant SFRC parameters defining the tensile behaviour. The intercept of Eq. 9 with the η-axis is η_u (= k), and can be written as a function of σ_R as:

$$\eta_u = 1 + \frac{2}{\sqrt{1-\sigma_R/f_{cm}}} \tag{10}$$

Likewise, Eq. 9 expressed as a function of η_u is:

$$\frac{\sigma_c}{f_{cm}} = 1 - \left(\frac{\eta-1}{\eta_u-1}\right)^2 \tag{11}$$

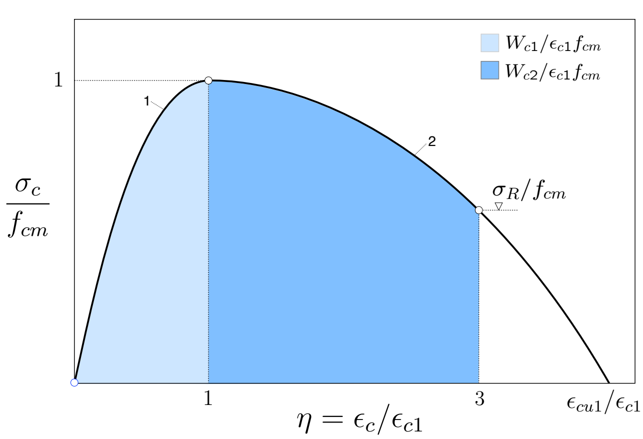

Figure 3. Schematic representation of the stress-strain relationship for SFRC previously proposed in [89–91].

Discussions within TG2 led to looking for an expression for the descending branch that allowed a very short description of the σ_c–ϵ_c model, with few or no new variables involved. This is why we opted for using Eq. 3 also for the second stretch of the new model since the curve is very similar to the parabola given by Eqs. 9 and 11. Eq. 3 has a maximum at η = 1 and intercepts the η-axis at $\eta = k$, and so it was only necessary to change the meaning of k after the peak, taking it as η_u (Eq. 10). Besides, detailed derivations using the response-surface methodology —a multivariate regression tool— applied to the database disclosed that σ_R depends mainly on the characteristic residual flexural strength for a crackmouth opening displacement of 0.5 mm, $f_{R,1k}$, the expression for it being:

$$\frac{\sigma_R}{f_{cm}} = 0.1839 + 0.02203\, f_{R,1k} \tag{12}$$

where $f_{R,1k}$ must be introduced in MPa (Eq. 16 in [91]). Such derivation was made by fitting the energy absorbed by the tests in the database between ϵ_{c1} and 3 ϵ_{c1}, W_{c2}, which is related to the residual compressive strength as:

$$\frac{\sigma_R}{f_{cm}} = \frac{3W_{c2}}{2f_{cm}\,\epsilon_{c1}} - 2 \tag{13}$$

Inserting Eq. 12 in Eq. 10 yields:

$$\eta_u = 1 + \frac{20}{\sqrt{82 - 2.2\, f_{R,1k}}} \tag{14}$$

which is the value that should be used for k in the descending stretch of the compressive stress-strain model given by Eq. 3.

3.2. Stress distribution in ULS

For the design of cross sections in ULS, EC2 Section 8.1.2 (1) [73] proposes using a parabola-rectangle stress distribution (see Figure 4c), defined as:

$$\eta_u = \begin{cases} f_{cd}\,[1-(1-\epsilon_c/\epsilon_{c2})^2] & \text{for} \quad 0 \le \epsilon_c \le \epsilon_{c2} \\ f_{cd} & \text{for} \quad \epsilon_{c2} \le \epsilon_c \le \epsilon_{cu} \end{cases} \tag{15}$$

where ϵ_{c2} and ϵ_{cu} are 0.0020 and 0.0035, respectively, for concrete without fibres. Alternatively, a rectangular stress block distribution as given in Figure 4d may be assumed, as stated in section 8.1.2 (2).

Annex L accounts for the enhancement of toughness and ductility in compression provided by the fibre by increasing the strains defining the stress distribution, ϵ_{c2} and ϵ_{cu}, to 0.0025 and 0.0060, respectively.

These new values for ϵ_{c2} and ϵ_{cu} for SFRC are based on the observed behaviour of the SFRCs in the database. In particular, the energy consumption up to ϵ_{c2} increases 45% in average compared to the corresponding base concrete (see Table 1). As fibres have little effect on the compressive strength, the toughness increase up to the peak of the parabola, and subsequently the new strain that corresponds with the peak, can be obtained by multiplying the strain for the peak stress of the base concrete —without fibres— times W°_{f1} (= W_{f1}/W_{c1}, see Table 1):

$$\epsilon_{f2} = \epsilon_{c2}\, W^{\circ}_{f1} \tag{16}$$

where ϵ_{f2} is the strain for the peak of the parabola for the concrete with fibres (we use subscript '*f*' instead of '*c*' to specify that we refer to concrete reinforced with steel fibres). The re-

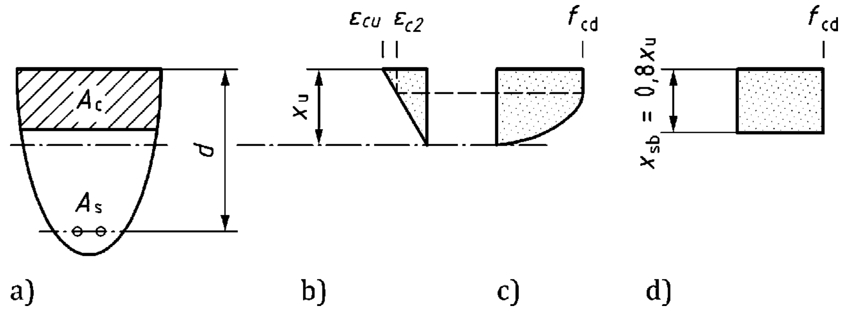

Figure 4. Stress distributions within the compression zone: a) cross section; b) assumed strain distribution; c) parabola-rectangle stress distribution; d) rectangular stress distribution. (Figure 8.2, EC2 [73])

sult is 0.0029, rounded down to 0.0025, which is finally taken as ϵ_{c2} for ULS calculations in SFRC.

Regarding the value for ϵ_{cu} with fibres, it is figured out by enforcing that the rectangular part consumes the same energy as the post-peak stretch of the new stress-strain curve (Eq. 9) up to 3 ϵ_{f2}. The energy consumed in this stretch is, on average, 2.83 W_{c1}, which is 183% more energy than consumed up to the peak by the corresponding base concrete, Table 1. For the parabola-rectangle law of Eq. 15, this can be expressed as:

$$W_{f2}^{\circ} = \frac{W_{f2}}{W_{c2}} = \frac{f_{fd}\,(\epsilon_{fu} - \epsilon_{f2})}{\frac{2}{3}\,f_{cd}\,\epsilon_{c2}} \qquad (17)$$

where again we use subscript 'f' instead of 'c' to refer to SFRC (for instance, ϵ_{fu} means ϵ_{cu} for the SFRC). As stated above, the strength increase due to fibres is small and can be neglected (i.e. $f_{fd} = f_{cd}$ in Eq. 17). Then:

$$W_{f2}^{\circ} = \frac{3}{2}\left(\frac{\epsilon_{fu}}{\epsilon_{f2}} - 1\right)\frac{\epsilon_{f2}}{\epsilon_{c2}} \qquad (18)$$

Table 1: Statistics of the unit toughness increase for SFRC.

	Mean	(Std. dev.)	[Min.–Max.]
$W_{f1}^{\circ}(=W_{f1}/W_{c1})$	1.45	(0.52)	[0.91–3.73]
$W_{f2}^{\circ}(=W_{f2}/W_{c2})$	2.83	(1.09)	[1.12–5.49]

where the ratio $\epsilon_{f2}/\epsilon_{c2}$ equals W_{f1}° (Eq.16). Then, solving for $\epsilon_{fu}/\epsilon_{f2}$ in Eq. 18 we get:

$$\frac{\epsilon_{fu}}{\epsilon_{f2}} = \frac{2}{3}\,\frac{W_{f2}^{\circ}}{W_{f1}^{\circ}} + 1 \qquad (19)$$

Introducing the values in Table 1 for W_{f1}° and W_{f2}° we get a ratio of 2.30. Taking ϵ_{f2} (= ϵ_{c2} for a SFRC) as 0.0029 (as derived above) we get that ϵ_{fu} (= ϵ_{cu} for a SFRC) is 0.0067, whereas for ϵ_{f2} = 0.0025 we obtain ϵ_{fu} = 0.0057. So, finally we round the result and take 0.0060 as the value of ϵ_{cu} for a SFRC.

Note that values for W_{f1}° and W_{f2}° in Table 1 are the average values of the stress-strain curves of the database disregarding dependencies on fibre content, fibre quality, etc., and we assume that the toughness of the parabola-rectangle curve for plain concrete increases according to them. In other words, we get ϵ_{c2} and ϵ_{cu} for an SFRC by enforcing that the parabola and the rectangle yield the same energy enhancement as the average of the curves in the database. Observe that absolutely none of the SFRC specimens in the compressive database broke before reaching a strain of 3 ϵ_{f1}, and most of them continued deforming way ahead of this value. Therefore, the mean values for W_{f1}° and W_{f2}° in Table 1 are on the safe side, and thus the new strain figures for SFRC in the curve defined in Eq. 15, namely 0.0025 and 0.0060, are on the safe side too.

4. DISCUSSION

4.1. Compressive and flexural SFRC classification

The new model for the compressive stress-strain behaviour in SFRC in Annex L allows a complete description of the material response, as can be seen graphically in Figure 5. The upper part plots the flexural stress versus the crack opening curves in non-dimensional format for several of the flexural performance classes (see Table 2, which reproduces Table L.2 of Annex L). These are called performance classes, but actually they only depend on the residual *flexural* strengths $f_{R,1k}$ and $f_{R,3k}$ experimentally determined according to EN 14651 [35]. The classification is based on a number —called SC (or σ_{SC} in this paper) for strength class— that corresponds to the minimum value required for $f_{R,1k}$ in MPa, and a letter associated to the ratio $f_{R,3k}/\sigma_{SC}$. For instance, class 4.0 b means that σ_{SC} = 4.0 MPa $\leq f_{R,1k} <$ 4.5 MPa and 0.7 $\leq f_{R,3k}/\sigma_{SC} <$ 0.9 (see Table 2).

The lower part of Figure 5 plots the new compressive stress-strain law in Annex L as described in Section 2 and explained in Section 3. The plot is in a non-dimensional format, the abscissa and ordinate representing ϵ_c/ϵ_{c1} (= η) and σ_c/f_{cm}, respectively. Note that the intercept of the curve with the horizontal axis is equal to η_u (=k). Since both ϵ_{c1} and k depend directly on $f_{R,1k}$ through Eqs. 1 and 2, respectively, it would seem that there is no reason to add any additional number or letter to the SFRC classification. However, an SFRC has to define the *compressive* class along with the flexural performance class since it is apparent that the *compressive* strength correlates with the residual flexural strengths. The new compressive model in Annex L does not contain information about this correlation per se, but the multivariate analyses reported in [89–91] provide it. There it was found that the expression for the residual compressive strength as a function of the flexural behaviour is:

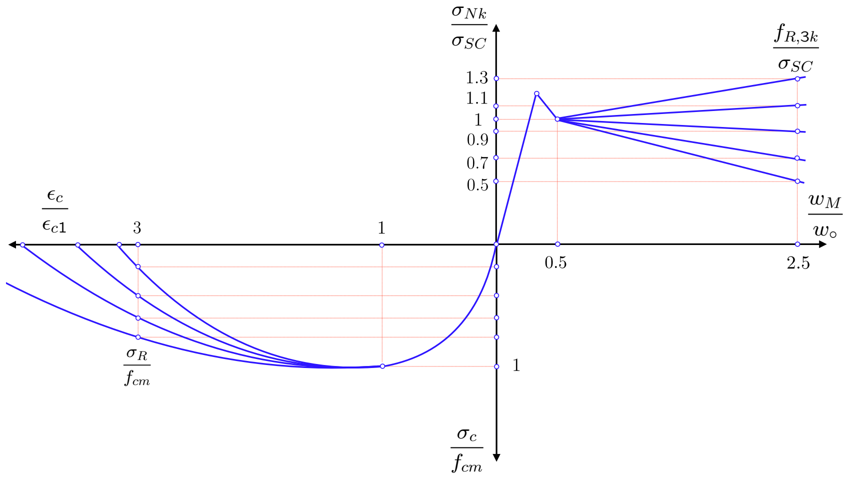

Figure 5. Description of the flexural/compression behaviour of SFRC and meaning of the material classification.

TABLE 2.
Performance classes for SFRC in MPa as defined in Table L.2 of EC2 [73].

Ductility classes	Strength classes SC ($f_{R,1k} \geq SC$)												Analytical formulae
	1.0	1.5	2.0	2.5	3.0	3.5	4.0	4.5	5.0	6.0	7.0	8.0	
a	0.5	0.8	1.0	1.3	1.5	1.8	2.0	2.3	2.5	3.0	3.5	4.0	$f_{R,3k} \geq 0.5\ SC$
b	0.7	1.1	1.4	1.8	2.1	2.5	2.8	3.2	3.5	4.2	4.9	5.6	$f_{R,3k} \geq 0.7\ SC$
c	0.9	1.4	1.8	2.3	2.7	3.2	3.6	4.1	4.5	5.4	6.3	7.2	$f_{R,3k} \geq 0.9\ SC$
d	1.1	1.7	2.2	2.8	3.3	3.9	4.4	5.0	5.5	6.6	7.7	8.8	$f_{R,3k} \geq 1.1\ SC$
e	1.3	2.0	2.6	3.3	3.9	4.6	5.2	5.9	6.5	7.8	9.1	10.4	$f_{R,3k} \geq 1.3\ SC$

TABLE 3.
Performance classes for SFRC related with their residual flexural and compressive strengths (in MPa).

Ductility classes		Strength classes SC ($f_{R,1k} \geq SC$)											
		1.0	1.5	2.0	2.5	3.0	3.5	4.0	4.5	5.0	6.0	7.0	8.0
a:	$f_{R,3k}$	0.5	0.8	1.0	1.3	1.5	1.8	2.0	2.3	2.5	3.0	3.5	4.0
	f_{cm}	22	25	28	30	32	35	36	37	40	43	46	48
	σ_R	4	5	6	7	8	9	10	11	12	13	15	17
b:	$f_{R,3k}$	0.7	1.1	1.4	1.8	2.1	2.5	2.8	3.2	3.5	4.2	4.9	5.6
	f_{cm}	31	34	36	38	40	42	43	45	46	49	51	53
	σ_R	6	7	8	9	10	11	12	13	14	15	17	19
c:	$f_{R,3k}$	0.9	1.4	1.8	2.3	2.7	3.2	3.6	4.1	4.5	5.4	6.3	7.2
	f_{cm}	40	42	44	46	47	49	50	51	53	55	56	58
	σ_R	8	9	10	11	12	13	14	15	16	17	19	21
d:	$f_{R,3k}$	1.1	1.7	2.2	2.8	3.3	3.9	4.4	5.0	5.5	6.6	7.7	8.8
	f_{cm}	49	51	52	53	55	56	57	58	59	60	62	63
	σ_R	10	11	12	13	14	15	15	16	17	19	21	23
e:	$f_{R,3k}$	1.3	2.0	2.6	3.3	3.9	4.6	5.2	5.9	6.5	7.8	9.1	10.4
	f_{cm}	58	59	60	61	62	63	64	64	65	66	67	68
	σ_R	12	13	14	15	15	16	17	18	19	21	23	25

$$\sigma_R = -1.77 + 1.807\, f_{R,1k} + 9.12\, \frac{f_{R,3k}}{f_{R,1k}} \tag{20}$$

where the residual flexural strengths are introduced in MPa to obtain σ_R in MPa. Both $f_{R,1k}$ and $f_{R,3k}$ are the only significant parameters to get σ_R. Interestingly, they are also the parameters defining the flexural performance class.

On the other hand, Eq. 12 already expresses the result obtained for σ_R/f_{cm}. It should be noted that only $f_{R,1k}$ was disclosed as a significant parameter to obtain the non-dimensional version of σ_R in Eq. 12. Combining Eqs. 12 and 20, the relation between the compressive strength and the residual flexural strengths follows as:

$$f_{cm} = \frac{-1.77 + 1.807\, f_{R,1k} + 9.12\, \dfrac{f_{R,3k}}{f_{R,1k}}}{0.1839 + 0.02203\, f_{R,1k}} \tag{21}$$

TABLE 4.
Performance classes for SFRC related with their relevant strains both for the parabola-rectangle model in ULS, ϵ_{f2} and ϵ_{fu}, and for the stress-strain general model, ϵ_{f1} and ϵ_{fu1}, (strains in ‰; SC in MPa).

Ductility classes		Strength classes SC ($f_{R,1k} \geq SC$)											
		1.0	1.5	2.0	2.5	3.0	3.5	4.0	4.5	5.0	6.0	7.0	8.0
a:	$\epsilon_{f2} = \epsilon_{f1}$	2.0	2.1	2.3	2.4	2.4	2.5	2.6	2.7	2.8	2.9	3.0	3.2
	ϵ_{fu}	5.0	5.3	5.6	5.9	6.1	6.3	6.6	6.8	7.0	7.4	7.7	8.1
	ϵ_{fu1}	6.6	7.0	7.4	7.7	8.1	8.4	8.7	9.0	9.3	9.9	10.4	11.0
b:	$\epsilon_{f2} = \epsilon_{f1}$	2.3	2.4	2.5	2.5	2.6	2.7	2.8	2.8	2.9	3.0	3.1	3.3
	ϵ_{fu}	5.6	5.9	6.1	6.3	6.5	6.7	6.9	7.1	7.3	7.7	8.0	8.4
	ϵ_{fu1}	7.4	7.7	8.0	8.3	8.6	8.9	9.2	9.5	9.8	10.3	10.8	11.4
c:	$\epsilon_{f2} = \epsilon_{f1}$	2.5	2.5	2.6	2.7	2.8	2.8	2.9	3.0	3.0	3.1	3.2	3.4
	ϵ_{fu}	6.1	6.3	6.5	6.7	6.9	7.1	7.3	7.4	7.6	8.0	8.3	8.6
	ϵ_{fu1}	8.0	8.3	8.6	8.9	9.1	9.4	9.7	9.9	10.2	10.7	11.2	11.7
d:	$\epsilon_{f2} = \epsilon_{f1}$	2.6	2.7	2.8	2.8	2.9	3.0	3.0	3.1	3.1	3.2	3.3	3.5
	ϵ_{fu}	6.5	6.7	6.9	7.1	7.2	7.4	7.6	7.7	7.9	8.2	8.6	8.9
	ϵ_{fu1}	8.5	8.8	9.1	9.3	9.6	9.8	10.1	10.3	10.6	11.1	11.6	12.1
e:	$\epsilon_{f2} = \epsilon_{f1}$	2.8	2.8	2.9	3.0	3.0	3.1	3.1	3.2	3.2	3.3	3.4	3.5
	ϵ_{fu}	6.9	7.0	7.2	7.4	7.5	7.7	7.9	8.0	8.2	8.5	8.8	9.1
	ϵ_{fu1}	9.0	9.3	9.5	9.7	10.0	10.2	10.4	10.7	10.9	11.4	11.9	12.4

where residual flexural strengths are introduced in MPa to obtain f_{cm} in MPa. This formula depends on the ratio $f_{R,3k}/f_{R,1k}$, and thus it is only valid for SFRC with hooked-end fibres since the database in [89–91] contain results for this type of SFRC only.

Equation 21 gives an estimate of the compressive strength needed to obtain a definite flexural performance class with SFRC with hooked-end fibres, defined by the desired residual flexural strengths. Table 3 arrays all the estimates given by Eqs. 20 and 21 for each flexural performance class of Annex L. In each cell of the matrix, we give the estimate for the compressive strength f_{cm} needed to obtain the desired flexural performance class along with an estimate for the residual compressive strength. For instance, Table 3 indicates that you need at least a C35/45 (whose minimum f_{cm} is 43 MPa) to produce a class 4.0 b, whereas the expected minimum value for σ_R is 12 MPa. So, the complete classification of this SFRC should be C35/45 4.0 b. It bears emphasis that obtaining flexural performance class 4.0 b with a compressive class below C35/45 may be rather difficult.

4.2. Ductility in compression

The deformability in compression of SFRCs of each performance class can be estimated using the new stress-strain model in Annex L. Indeed, Eqs. 1 and 2 allow obtaining ϵ_{c1} and ϵ_{cu1} values for each flexural performance class, see Table 4 (we use subscript 'f' instead of 'c' to name parameters of a SRFC). Note that these strain values depend jointly on the compressive strength and the residual flexural strengths.

As aforementioned, Annex L follows the core of EC2 [73] in providing two constant values for the strains determining the parabola-rectangle used in ULS, namely ϵ_{f2} and ϵ_{fu} (again, subscript 'f' is for SFRC). It is done so for the sake of brevity and consistency since mirroring the structure of EC2 [73] for plain concrete avoids new formulas or parameters and subsequent definitions. However, it is also possible to give defining strains for the parabola-rectangle model for each performance class. It is appropriate to do so since ULS calculations may also benefit from having selected a flexural performance class for the SFRC element or structure under study. To do this, we assume that ϵ_{f2} takes the same value as ϵ_{f1}. Then, we can use Eq. 19 to calculate ϵ_{fu} for each class, but in its dimensional version:

$$\frac{\epsilon_{fu}}{\epsilon_{f2}} = \frac{2}{3}\frac{W_{f2}}{W_{f1}} + 1 \tag{22}$$

where W_{f1} and W_{f2} are now calculated with the complete stress-strain model (Subsection 3.1) but assuming that the up and down stretches are perfect parabolas. Additionally, as W_{f2} is the energy per unit volume absorbed between ϵ_{f1} and 3 ϵ_{f1}, we assume that the detracted area between 3 ϵ_{f1} and k ϵ_{f1} can be calculated as if it was a triangle. The result for ϵ_{fu} is:

$$\frac{\epsilon_{fu}}{\epsilon_{f2}} = \frac{2}{3}\left((k-1) - \frac{3}{4}(k-3)\frac{\sigma_R}{f_{cm}}\right) + 1 \tag{23}$$

where k is the value for the downward stretch of the curve (Eq. 2), which coincides with the nondimensional strain of the intercept with the abscissa ($k = \eta_u$). Table 4 arrays the results of Eq. 23 for each performance class.

The constant values for ϵ_{f2} and ϵ_{fu} that Annex L, section L.8.1 (4), proposes, namely 0.0025 and 0.0060, roughly coincide with these of classes 3.0 a, 2.0 b, and 1.0 c. So, using the proposed constant strains leads to slightly overestimating the ductility for weaker classes and underestimating it for the stronger ones, actually the majority of them. For instance, these strains for class 1.0 a are 0.0020 and 0.0050, whereas for class 8.0 e are 0.0035 and 0.0091. It bears emphasis that all these strain values are on the safe side since absolutely none of the SFRC specimens in the compressive database broke before reaching a strain of 3ϵ_{f1}, and most of them continued deforming way ahead this value [89–91].

4.3. Outlook about the impact of SFRC ductility on Eurocode 4

The benefits of an increased concrete ductility conferred by the addition of steel fibre reinforcement have consequences

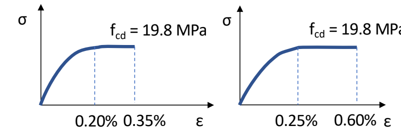

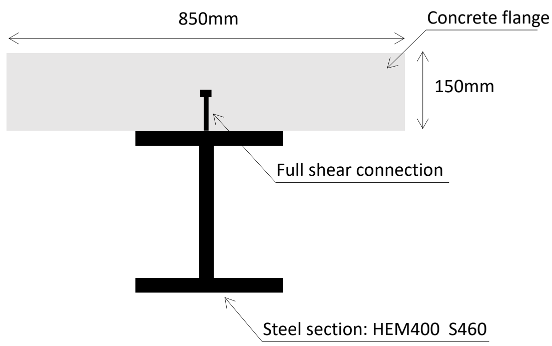

ULS Sagging bending resistance	Normal concrete slab C35/45	SFRC slab C35/45 4.0b
Full-plastic resistance:	*3132 kNm*	
Simplified method: EN1994-1-1 (2005)	2662 kNm *(Reference)*	
Simplified method: prEN1994-1-1 (2021)	2818 kNm **+5.9%**	
Advanced method: prEN1994-1-1 (2021)	2864 kNm **+7.6%**	3071 kNm **+15.4%**

Figure 6. Steel-concrete composite section considered in the example.

which reach beyond concrete structures according to Eurocode 2 [27]. For instance, the maximum compression strain of plain concrete in concrete (ϵ_{cu} = 0.0035 for normal strength concrete in accordance with Eurocode 2 [27] and EC2 [73]) plays a relevant role also for the design of steel-concrete composite structures in accordance with Eurocode 4 [93].

For several composite cross-section configurations in fact the concrete component may reach its ultimate compressive strain before the structural steel component develops enough strain to reach yielding in most of the steel section, thus full plastic capacity may not be reached.

This aspect is explicitly considered when the strain-based resistance of the cross-section is performed (a recent review of strain-limited design method for composite beam sections is given by Zhang [71] and Schäfer *et al.* [72]). The described phenomenon depends on different effects that impact the rotation capacity, as the position of the plastic neutral axis, material strength and geometry of the cross-section. Thus when reaching the concrete ultimate strain before the plastic moment resistance of the steel section is attained, a concrete compression failure may occur in the compression zone even if the cross-section satisfies the Class 2 requirements (criteria to prevent local buckling effects in the steel sections prior to reaching of the plastic resistance, EN1993-1-1 [94]). On a general basis, a strain-based resistance with the stress-strain curves in accordance with EN 1992-1-1 [27] for concrete and reinforcement steel and EN1993-1-1 [94] for the stress-strain curve of structural steel would be required to consider the limited rotation capacity of the section due to the restrictions by the concrete. In addition, for composite beams with partial shear interaction, the strain discontinuity appearing in the composite connection shall be considered. To avoid this effort for practical design, Eurocode 4 [93] provides a simplified design method based on the full-plastic cross-section moment resistance introducing a reduction factor β. The reduction factors were derived by a large parametric study comparing the plastic and strain-limited resistance for a large spectrum of composite cross-sections and material combinations. For current Eurocode 4 [93] this study was provided by Hanswille *et al.* [95] and newer investigation for the second generation of Eurocode 4, prEN1994-1-1 [96], can be found in Schäfer *et al.* [97].

Furthermore, the use of steel grades such as S500 or higher (already foreseen in product standards [98], design codes for steel structures and the second generation of Eurocodes) requires developing higher strains to reach yielding. At increasing strain the cases of premature compression concrete failure become even more relevant, reducing the interest of high steel strength with composite structures.

The following configurations may lead to a limitation of the plastic moment resistance (a more detailed discussion of the configurations is given in [99]):

1. composite beam with a limited effective width of the concrete flange (e.g. edge beams, due to openings in the slab, use of precast slab elements);
2. composite beams with high strength steel (in particular for S420 or higher grades);
3. composite beams with an intensive concrete contribution (e.g. for partially encased composite beams with a large amount of reinforcement, fully encased composite beams such as filler beam decks and shallow-floor beams);
4. composite beams with asymmetric steel sections having a bottom flange area significantly higher than the top flange;
5. composite beams with hybrid steel sections having a bottom flange resistance significantly higher than the top flange;
6. concrete encased composite columns without external steel tube.

To quantify the impact that higher concrete ductility obtained by steel fibre reinforcement would bring for steel-concrete composite structures a calculation example is proposed corresponding to case 2 of above list. A typical composite beam cross-section with a standard profile and a concrete flange on top of the upper steel flange is considered (see Figure 6). Complete interaction with full shear connection is assumed. The example considers sagging bending moment, therefore with the concrete component being entirely under compression.

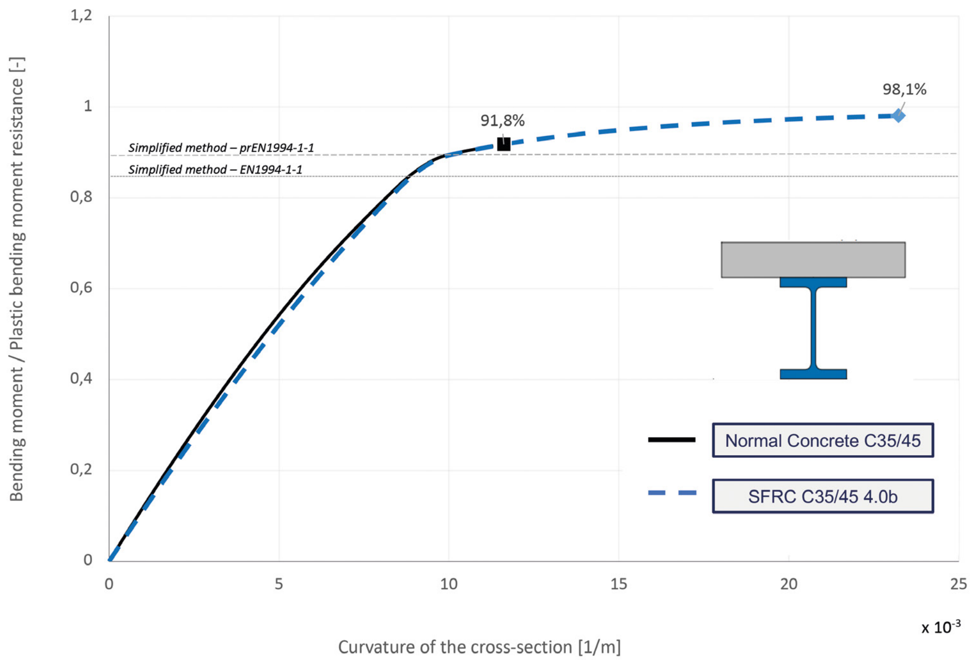

Figure 7. Moment-curvature diagram of the cross-section of Figure 6 with different types of concrete slab.

The simplified method is based on a plastic stress block distribution assuming the whole cross-section attaining the plastic resistance, whereas the reduction factor β for the deep-lying neutral axis is applied as in the current design provisions of current Eurocode 4 [93] for the normal strength concrete. The simplified method is also applied with the reduction factor β proposed in the future version of the design code based on Schäfer *et al.* [97].

The advanced method foresees an integration of the material laws over the cross-section. The calculation is performed both with the non-linear stress-strain relationship according to subsection 3.1 as well as for the parabola rectangle explained in subsection 3.2, and with f_{cd} obtained following the provisions in the draft of the new Eurocode 4 [96] for calculation of the resistance of a cross-section of this type [97], for a compressive strength class C35/45. The results have a maximum difference of 2% (the energy consumption of both models is the same for the selected class C35/45 4.0 b) and for sake of simplicity only the ones obtained with the parabola-rectangle are reported in Figure 6. For the steel material, the quadrilinear stress-strain relationship has been used according to [97].

Since steel is very ductile and can reach very large elongations before rupture, in this kind of cross-sections under sagging bending moment the maximum resistance is reached when the top fibre attains the maximum admissible concrete compressive strain (ultimate strain). Figure 7 shows that beside an improvement of the bending moment resistance, a remarkable increase of the section ductility is achieved. This leads to significant higher cross-section rotation capacity in plastic hinges when using SFRC than the one of plain concrete thanks to a pronounced yielding plateau which is more than doubled. The beneficial effects of this increased ductility will not be discussed here, but is focus of ongoing research and is hinted that it may contribute in redistributing bending moments in continuous systems and ensuring ductility of specific shear connection configurations.

As a conclusion, the increased concrete ductility achieved by SFRC in compression is promising for the optimization of some specific steel-concrete composite structures. For a future deployment of higher strengths for the structural steel sections (both for columns and beam applications) and the more and more widespread use of cross-section configuration with limited rotation capacity an increased concrete ductility appears essential.

It shall be reminded that the considerations exposed in this chapter have focused on the impact of the improved compression behaviour of SFRC compared to concrete without fibres: other advantages are of course expected by the improved tensile behaviour (crack limitation, durability, shear connection resistance), possibly an additional reason to combine these materials in steel-concrete composite structures.

5. CONCLUSIONS

Annex L of the new EC2 [73] considers the enhancement in ductility and toughness in compression due to fibres. It proposes to use the same stress-strain formulas for the compressive behaviour of plain concrete in the core of EC2 [73] but changes the strain parameters to account for the ductility increase. In particular, parameter k is used to define the initial slope of the curve in the ramp-up stretch, up to the stress peak, but changes after the peak to represent the intercept of the downward curve with the strain axis, and so it defines the energy consumption of the material after the peak. Similarly, Annex L also enlarges the strain values needed for the ULS calculation of SFRC sections. In this paper, we give detailed derivations of all the expressions in Annex L related to the compressive SFRC behaviour, which are based on a multivariate analysis of a large database [89–91].

In addition, we provide formulas to calculate the compressive strength needed to get a desired flexural performance class since the compressive behaviour of a base concrete is correlated with the residual flexural strengths of the corresponding SFRC. We give compressive strength values for each flexural performance class defined in Annex L of the new EC2 [73], which may be very useful to design a SFRC.

Regarding the strain values for ULS calculations, Annex L mirrors the approach for plain concrete and gives constant values of the parameters defining the parabola-rectangle model, ϵ_{c2} and ϵ_{cu}, for any SFRC. However, we propose particular values of these parameters for each flexural performance class, to take better advantage of the ductility increase of SFRC in stronger classes.

Finally, we highlight the importance of accounting for the real SFRC ductility in composite structures since the low deformation capacity of plain concrete makes that steel elements cannot be used to their limits. We provide an example of a composite beam with a deep neutral axis and high steel strength, which resists 15.4% more load and duplicates its rotation capacity with the new provisions in Annex L.

Acknowledgements

The authors gratefully acknowledge the financial support from the *Ministerio de Ciencia e Innovación*, Spain, through grants PID2019-110928RB-C31 and RTC- 2017-6736-3, and the *Junta de Comunidades de Castilla-La Mancha*, Spain, through grant SBPLY/19/180501/000220.

Nomenclature

CMOD	Crack mouth opening displacement
E_{cm}	Mean elastic modulus of concrete/SFRC in 150 300 mm² cylinders
EC2	New Eurocode 2 (final draft, version 2022-11) [73]
f_{cd}	Design value of concrete/SFRC compressive strength
f_{fd}	Design value of SFRC compressive strength[1]
f_{cm}	Mean compressive strength of concrete/SFRC in 150 x 300 mm² cylinders
$f_{R,1k}$	Characteristic residual flexural strength for a crack mouth opening displacement of 0.5 mm
$f_{R,3k}$	Characteristic residual flexural strength for a crack mouth opening displacement of 2.5 mm
k	Coefficient
SC	Strength class
SFRC	Steel-fibre reinforced concrete
ULS	Ultimate limit state
W_{c1}	Volumetric deformation work in pre-peak branch of concrete/SFRC in 150 × 300 mm² cylinders (from $\epsilon_c = 0$ to $\epsilon_c = \epsilon_{c1}$)
W_{c2}	Volumetric deformation work in post-peak branch of concrete/SFRC in 150×300 mm² cylinders (from $\epsilon_c = \epsilon_{c1}$ to $\epsilon_c = \epsilon_{cu1}$)
W_{f1}	Volumetric deformation work in pre-peak branch of SFRC in 150 × 300 mm² cylinders (from $\epsilon_f = 0$ to $\epsilon_f = \epsilon_{f1}$)
W_{f2}	Volumetric deformation work in post-peak branch of SFRC in 150 × 300 mm² cylinders up to 3 ϵ_{f1} (from ϵ_{f1})
$W^{\circ}_{f1} = \frac{W_{f1}}{W_{c1}}$	Non-dimensional volumetric deformation work in pre-peak branch of SFRC
$W^{\circ}_{f2} = \frac{W_{f2}}{W_{c2}}$	Non-dimensional volumetric deformation work in post-peak branch of SFRC
w_M	Crack mouth opening displacement, CMOD
$w_{\circ}$=1mm	Coefficient to keep non-dimensionality
ϵ_c	Compressive strain in concrete/SFRC
ϵ_{c1}	Compressive strain in concrete/SFRC when the stress reaches the compressive strength in the stress-strain model for non-linear analysis
ϵ_{cu1}	Ultimate compressive strain in concrete/SFRC in the stress-strain model for non-linear analysis
ϵ_{c2}	Compressive strain in concrete/SFRC when the stress reaches the compressive strength in the ULS model
ϵ_{cu}	Ultimate compressive strain in concrete/SFRC in the ULS model
ϵ_f	Compressive strain in SFRC
ϵ_{f1}	Compressive strain in SFRC when the stress reaches the compressive strength in the stress-strain model for non-linear analysis
ϵ_{f2}	Compressive strain in SFRC when the stress reaches the compressive strength in the ULS model
ϵ_{fu}	Ultimate compressive strain in SFRC in the ULS model
ϵ_{fu1}	Ultimate compressive strain in SFRC in the stress-strain model for non-linear analysis
$\eta = \frac{\epsilon_c}{\epsilon_{c1}}$	Non-dimensional compressive strain in concrete/SFRC
$\eta_u = \frac{\epsilon_{cu1}}{\epsilon_{c1}}$	Non-dimensional ultimate compressive strain in concrete/SFRC in the stress-strain model for non-linear analysis
σ_c	Stress in concrete/SFRC
σ_{cd}	Design value of compressive stress in concrete/SFRC
σ_f	Stress in SFRC
σ_{Nk}	Characteristic nominal/flexural stress
σ_R	Compressive residual strength
σ_{SC}	Strength class, SC

1 Annex L does not use parameters with subscript f for referring to SFRC but uses subscript c for plain concrete and SFRC. However, the complete definition and derivation of the compressive model need to differentiate between both types of materials since we require to refer to a base concrete (c) and the SFRC resulting from reinforcing it with steel fibres (f).

References

[1] G. Tiberti, F. Germano, A. Mudadu, G. Plizzari, An overview of the flexural post–cracking behavior of steel fiber reinforced concrete, Structural Concrete 19 (2018) 695–718. https://doi.org/10.1002/suco.201700068

[2] N. Buratti, B. Ferracuti, M. Savoia, Concrete crack reduction in tunnel linings by steel fibre–reinforced concretes, Construction and Building Materials 44 (2013) 249–259. https://doi.org/10.1016/j.conbuildmat.2013.02.063

[3] M. di Prisco, G. Pizzari, L. Vandewalle, Fibre reinforced concrete: New design perspectives, Materials and Structures 42 (9) (2009) 1261–1281. https://doi.org/10.1617/s11527-009-9529-4

[4] F. Altun, T. Haktanir, K. Ari, Effects of steel fiber addition on mechanical properties of concrete and RC beams, Construction and Building Materials 21 (2007) 654–661. https://doi.org/10.1016/j.conbuildmat.2005.12.006
[5] B. Xu, H. Shi, Correlations among mechanical properties of steel fiber reinforced concrete, Construction and Building Materials 23 (12) (2009) 3468–3474. https://doi.org/10.1016/j.conbuildmat.2009.08.017
[6] S. Lee, C. J.Y., F. Vecchio, Simplified diverse embedment model for steel fiber–reinforced concrete elements in tension, ACI Materials Journal 110 (4) (2013) 403–412.
[7] A. Naaman, H. Reinhardt, High performance fiber reinforced cement composites–HPFRCC4, in: A. Naaman, H. Reinhardt (Eds.), RILEM Proceedings, PRO 30, RILEM Publications SARL, 2003.
[8] J. Walraven, Fibre reinforced concrete: A material in development, in: Conference in Structural Applications of Fiber Reinforced Concretes, Barcelona, Spain, 2007, pp. 199–213.
[9] Fibre reinforced concrete: Challenges and opportunities, in: J. Barros (Ed.), 8th RILEM International Symposium (BEFIB 2012), Guimaraes, Portugal, RILEM Publications SARL, 2012.
[10] J. Deluce, F. Vecchio, Cracking behavior of steel fiber–reinforced concrete members containing conventional reinforcement, ACI Structural Journal 110 (3) (2013) 481–490.
[11] A. Caratelli, A. Meda, Z. Rinaldi, Design according to MC2010 of a fibre–reinforced concrete tunnel in Monte Lirio, Panama, Structural Concrete 13 (3) (2012) 166–173. https://doi.org/10.1002/suco.201100034
[12] A. De La Fuente, P. Pujadas, A. Blanco, A. Aguado, Experiences in Barcelona with the use of fibres in segmental linings, Tunnelling and Underground Space Technology 27 (1) (2012) 60–71. https://doi.org/10.1016/j.tust.2011.07.001
[13] H. Mashimo, N. Isago, T. Kitani, T. Endou, Effect of fiber reinforced concrete on shrinkage crack of tunnel lining, Tunnelling and Underground Space Technology 21 (3–4) (2006) 382–3.
[14] H. Mashimo, N. Isago, T. Kitani, Numerical approach for design of tunnel concrete lining considering effect of fiber reinforcements, Tunnelling and Underground Space Technology 19 (4–5) (2004) 454–5.
[15] L. Sorelli, F. Toutlemonde, On the design of steel fibre reinforced concrete tunnel lining segments, in: XI International Conference on Fracture. Turin, Italy, 2005.
[16] R. Gettu, B. Barragán, T. García, J. Ortiz, R. Justa, Fiber concrete tunnel lining, Concrete International 28 (8) (2006) 63–69.
[17] G. Tiberti, G. Plizzari, J. Walraven, C. Blom, Concrete tunnel segments with combined traditional and fibre reinforcement, in: Tailor Made Concrete Structures – New Solutions for Our Society (*fib* Symposium). Amsterdam, The Netherlands, 2008, pp. 605–610.
[18] R. Burgers, J. Walraven, G. Plizzari, G. Tiberti, Structural behaviour of SFRC tunnel segments during TBM operations, in: World Tunnel Congress ITA-AITES. Prague, Czech Republic, 2007, pp. 1461–1467.
[19] T. Kasper, C. Edvardsen, G. Wittneben, D. Neumann, Lining design for the district heating tunnel in Copenhagen with steel fibre reinforced concrete segments, Tunnelling and Underground Space Technology 23 (5) (2008) 574–587.
[20] A. Caratelli, A. Meda, Z. Rinaldi, P. Perruzza, P. Romualdi, Precast tunnel segment in fibre reinforced concrete., in: Concrete Engineering for Excellence and Efficiency (*fib* Symposium). Prague, Czech Republic, 2011, pp. 579–582.
[21] A. Meda, G. Plizzari, A new design approach for SFRC slabs on grade based on fracture mechanics, ACI Structural Journal 101 (3) (2004) 298–303. https://doi.org/10.14359/13089
[22] B. Belletti, R. Cerioni, A. Meda, G. Plizzari, Design aspects on steel fiber reinforced concrete pavements, Journal of Materials in Civil Engineering 20 (9) (2008) 599–607. https://doi.org/10.1061/(ASCE)0899-1561(2008)20:9(599)
[23] J. Michels, D. Waldmann, S. Maas, A. Zürbes, Steel fibers as only reinforcement for flat slab construction – Experimental investigation and design, Construction and Building Materials 26 (1) (2012) 145–155. https://doi.org/10.1016/J.CONBUILDMAT.2011.06.004
[24] M. Soutsos, T. Le, A. Lampropoulos, Flexural performance of fibre reinforced concrete made with steel and synthetic fibres, Construction and Building Materials 36 (2012) 704–710. https://doi.org/10.1016/j.conbuildmat.2012.06.042
[25] A. De La Fuente, R. Escariz, A. De Figueiredo, C. Molins, A. Aguado, A new design method for steel fibre reinforced concrete pipes, Construction and Building Materials 30 (2012) 547–555. https://doi.org/10.1016/j.conbuildmat.2011.12.015
[26] *fib* Bulletins 65 & 66, Model Code 2010, Final Draft, International Federation for Structural Concrete, *fib*. Lausanne, Switzerland, 2012.
[27] EN 1992-1-1, Eurocode 2: Design of Concrete Structures, European Committee for Standardization–CEN, 2020.
[28] UNI 11039-2, Steel Fibre Reinforced Concrete–Test Method for Determination of First Crack Strength and Ductility Indexes, Italian Standardization Body– UNI, 2003.
[29] Guide for the Design and Construction of Fiber–Reinforced Concrete Structures, Italian Standardization Body–UNI, 2003.
[30] DAfStb TR SFRC Draft, DAfStb Technical Rule on Steel Fibre Reinforced Concrete, Deutscher Ausschuss für Stahlbeton (DAfStb), 2012.
[31] EHE 08, Instrucción de Hormigón Estructural, Ministerio de Fomento. Secretaría General Técnica, 2008.
[32] RILEM TC 162 TDF, Test and design methods for steel fibre reinforced concrete. Design of steel fibre reinforced concrete using the σ w method: Principles and applications, Materials and Structures 35 (5) (2002) 262–278.
[33] RILEM TC 162 TDF, Test and design methods for steel fibre reinforced concrete. $\sigma - \epsilon$ design method. Final recommendation, Materials and Structures 36 (8) (2003) 560–567.
[34] RILEM TC 162 TDF, Test and design methods for steel fibre reinforced concrete. $\sigma - \epsilon$ design method. Recommendation, Materials and Structures 33 (2) (2000) 75–81.
[35] EN14651, Test Method for Metallic Fibre Concrete–Measuring the Flexural Tensile Strength (Limit of Proportionally (LOP), Residual), European Committee for Standardization, Brussels, 2005.
[36] D. Yoo, N. Banthia, Experimental and numerical analysis of the flexural response of amorphous metallic fiber reinforced concrete, Materials and Structures 50 (64) (2017).
[37] S. Yazici, G. Inan, V. Tabak, Effect of aspect ratio and volume fraction of steel fiber on the mechanical properties of SFRC, Construction and Building Materials 21 (2007) 1250–1253. https://doi.org/10.1016/j.conbuildmat.2006.05.025
[38] R. Swamy, P. Mangat, A theory for the flexural strength of steel fiber reinforced concrete, Cement and Concrete Research 4 (2) (1974) 313–325.
[39] J. Olesen, Crack propagation in fiber–reinforced concrete beams, Journal of Engineering Mechanics 127 (3) (2001) 272–280. https://doi.org/10.1061/(ASCE)0733-9399(2001)127:3(272)
[40] M. Pajak, T. Ponikiewski, Flexural behavior of self–compacting concrete reinforced with different types of steel fibers, Construction and Building Materials 47 (2013) 397–408. https://doi.org/10.1016/j.conbuildmat.2013.05.072
[41] D. Yoo, N. Banthia, J. Yang, Y. Yoon, Mechanical properties of corrosion–free and sustainable amorphous metallic fiber–reinforced concrete, ACI Materials Journal 113 (5) (2016) 633–643. https://doi.org/10.14359/51689108
[42] P. Marti, T. Pfyl, V. Sigrist, T. Ulaga, Harmonized test procedures for steel fiber–reinforced concrete, ACI Materials Journal 96 (6) (1999) 676–686. https://doi.org/10.14359/794
[43] P. Stroeven, Stereological principles of spatial modeling applied to steel fiber– reinforced concrete in tension, ACI Materials Journal 106 (3) (2009) 213–222.
[44] J. Voo, S. Foster, Variable engagement model for fibre reinforced concrete in tension, in: Uniciv Report R–420. School of Civil and Environmental Engineering, University of New South Wales, Sydney, NSW, Australia, 2003, pp. 86–96.
[45] T. Leutbecher, E. Fehling, Crack width control for combined reinforcement of rebars and fibers exemplified by ultra–high–performance concrete, in: Uniciv Report R–420. School of Civil and Environmental Engineering, fib Task Group 8.6, Ultra High Performance Fiber Reinforced Concrete–UHPFRC, 2008, pp. 1–28.
[46] S. Lee, J. Cho, F. Vecchio, Diverse embedment model for steel fiber–reinforced concrete in tension: Model development, ACI Materials Journal 108 (5) (2011) 516–525.
[47] S. Lee, J. Cho, F. Vecchio, Diverse embedment model for steel fiber–reinforced concrete in tension: Model verification, ACI Materials Journal 108 (5) (2011) 526–535.
[48] ACI 544.4R-88, Design Considerations for Steel Fiber Reinforced Concrete, Tech. rep., American Concrete Institute (1999).
[49] S. Shah, P. Stroeven, D. Dalhuisen, P. Van Stekelenburg, Complete stress–strain curves for steel fibre reinforced concrete in uniaxial tension and compression, Testing and Test Methods of Fibre Cement Composites (1978) 399– 408.
[50] M. A. Tasdemir, A. Ilki, M. Yerlikaya, Mechanical behaviour of steel fibre reinforced concrete used in hydraulic structures, in: International Conference of Hydropower and Dams, HYDRO 2002, 2002, pp. 159–166.
[51] F. Bayramov, M. A. Tasdemir, A. Ilki, M. Yerlikaya, Steel fibre reinforced concrete for heavy traffic load conditions, in: 9th International Symposium on Concrete Roads, 2004, pp. 73–82.
[52] L. Hsu, C. Hsu, Complete stress–strain behavior of high–strength concrete under compression, Magazine of Concrete Research 46 (169) (1994) 301–312. http://dx.doi.org/10.1680/macr.1994.46.169.301

[53] A. Someh, N. Saeki, Prediction for the stress–strain curve of steel fiber reinforced concrete, in: Proceedings Japan Concrete Institute, Vol. 18, 1994, pp. 1149–1154.
[54] M. Mansur, M. Chin, T. Wee, Stress–strain relationship of high–strength fiber concrete in compression, ASCE Journal of Materials in Civil Engineering 11 (1999) 21–29. https://doi.org/10.1061/(ASCE)0899-1561(1999)11:1(21)
[55] M. Nataraja, N. Dhang, A. Gupta, Stress–strain curves for steel–fiber reinforced concrete under compression, Cement and Concrete Composites 21 (5–6) (1999) 383–390. https://doi.org/10.1016/S0958-9465(99)00021-9
[56] R. Neves, J. Fernandes de Almeida, Compressive behaviour of steel fibre reinforced concrete, Structural Concrete 6 (1) (2005) 1–8. https://doi.org/10.1680/stco.2005.6.1.1
[57] J. Barros, J. Figueiras, Flexural behavior of SFRC: Testing and modeling, Journal of Materials in Civil Engineering 11 (4) (1999) 331–339. https://doi.org/10.1061/(asce)0899-1561(1999)11:4(331)
[58] R. Neves, Modelling the Compressive Behaviour of Steel Fibre Reinforced Concrete, Master Thesis, Instituto Superior Técnico, Lisbon, 2000.
[59] D. Fanella, A. Naaman, Stress-strain properties of fiber reinforced mortar in compression, ACI Journal 82 (4) (1985) 475–483.
[60] D. Otter, A. E. Naaman, Steel fibre reinforced concrete under static and cyclic compressive loading, in: RILEM Symposium FRC 86, Devel. in Fibre Reinforced Cement and Concrete, Vol. 1, 1986.
[61] K. Marar, O. Eren, T.Çelik, Relationship between impact energy and compression toughness energy of high-strength fiber-reinforced concrete, Materials Letters 47 (2001) 297–304.
[62] J. Thomas, A. Ramaswamy, Mechanical properties of steel fiber-reinforced concrete, Journal of Materials in Civil Engineering 19 (2007) 385–392. https://doi.org/10.1061/(ASCE)0899-1561(2007)19:5(385)
[63] L. Daniel, A. Loukili, Behavior of high–strength fiber–reinforced concrete beams under cyclic loading, ACI Structural Journal 99 (3) (2002) 248–256. https://doi.org/10.14359/11908
[64] G. Williamson, The effect of steel fibers on the compressive strength of concrete, in: Fiber Reinforced Concrete – ACI Symposium Publication, Vol. 44, American Concrete Institute, 1974, pp. 195–207.
[65] P. Soroushian, C. Lee, Constitutive modeling of steel fiber reinforced concrete under direct tension and compression, in: Fibre Reinforced Cements and Concretes, Recent Developments. University of Wales, College of Cardiff, School of Engineering, United Kingdom, 1989, pp. 363–375.
[66] A. Ezeldin, P. Balaguru, Normal and high strength fiber reinforced concrete under compression, Journal of Materials in Civil Engineering 4 (4) (1992) 415–429. https://www.doi.org/10.1061/(ASCE)0899-1561(1992)4:4(415)
[67] Y. Ou, M. Tsai, K. Liu, K. Chang, Compressive behavior of steel fiber reinforced concrete with a high reinforcing index, Journal of Materials in Civil Engineering 24 (2) (2011) 207–215. https://doi.org/10.1061/(ASCE)MT.1943-5533.0000372
[68] L. Taerwe, Influence of steel fibres on strain–softening of high–strength concrete, Materials Journal 88 (6) (1992) 54–60. http://hdl.handle.net/1854/LU-204450
[69] B. Hughes, N. Fattuhi, Stress–strain curves for fiber reinforced concrete in compression, Cement and Concrete Research 7 (2) (1977) 173–183. https://doi.org/10.1016/0008-8846(77)90028-X
[70] F. Bencardino, L. Rizzuti, G. Spadea, Experimental tests vs. theoretical modeling for FRC in compression, FraMCoS, 2007, pp. 159–166.
[71] Q. Zhang, Moment and Longitudinal Resistance for Composite Beams Based on Strain Limited Design Method, Ph.D. thesis, Université du Luxembourg (2020).
[72] M. Schäfer, Q. Zhang, M. Braun, M. Banfi, Limitations of plastic bending resistance for composite beams deviated from strain-limitation, Journal of Constructional Steel Research 180 (2021) 106562. https://doi.org/10.1016/j.jcsr.2021.106562
[73] CEN, Eurocode 2, Design of concrete structures. Part 1-1: General rules – Rules for buildings, bridges and civil structures, prEN 1992-1-1: 2022, version of November 10, 2022, available at both UNE and CEN websites (2022).
[74] S. Lee, J. Oh, J. Cho, Compressive behavior of fiber-reinforced concrete with end-hooked steel fibers, Materials 8 (4) (2015) 1442–1458. https://doi.org/10.3390/ma8041442
[75] F. Bencardino, L. Rizzuti, G. Spadea, R. Swamy, Stress-strain behavior of steel fiber-reinforced concrete in compression, Journal of Materials in Civil Engineering 20 (2008) 255–263.
[76] P. Song, S. Hwang, Mechanical properties of high-strength steel fiber-reinforced concrete, Construction and Building Materials 18 (9) (2004) 669–673. https://doi.org/10.1016/j.conbuildmat.2004.04.027
[77] F. Bayramov, C. Tasdemir, M. Tasdemir, Optimisation of steel fibre reinforced concretes by means of statistical response surface method, Cement and Concrete Composites 26 (2004) 665–675. https://doi.org/10.1016/S0958-9465(03)00161-6
[78] B. Jo, Y. Shon, Y. Kim, The evaluation of elastic modulus for steel fiber reinforced concrete, Russian Journal of Nondestructive Testing 37 (2001) 152– 161. https://doi.org/10.1023/A:1016780124443
[79] F. Aslani, S. Nejadi, Self-compacting concrete incorporating steel and polypropylene fibers: Compressive and tensile strengths, moduli of elasticity and rupture, compressive stress–strain curve, and energy dissipated under compression, Composites Part B: Engineering 53 (2013) 121–133. https://doi.org/10.1016/j.compositesb.2013.04.044
[80] Y. Şahin, F. Köksal, The influences of matrix and steel fibre tensile strengths on the fracture energy of high-strength concrete, Construction and Building Materials 25 (4) (2011) 1801–1806. https://doi.org/10.1016/j.conbuildmat.2010.11.084
[81] P. Cachim, J. Figueiras, P. Pereira, Fatigue behavior of fiber-reinforced concrete in compression, Cement and Concrete Composites 24 (2) (2002) 211–217.
[82] B. Barragán, R. Gettu, M. Martín, R. Zerbino, Uniaxial tension test for steel fibre reinforced concrete — A parametric study, Cement and Concrete Composites 25 (7) (2003) 767–777. https://doi.org/10.1016/S0958-9465(02)00096-3
[83] A. Medeiros, X. Zhang, G. Ruiz, R. Yu, M. de Souza Lima Velasco, Effect of the loading frequency on the compressive fatigue behavior of plain and fiber reinforced concrete, International Journal of Fatigue 70 (2015) 342–350. https://doi.org/10.1016/j.ijfatigue.2014.08.005
[84] H. Dhonde, Y. Mo, T. Thomas, C. Hsu, J. Vogel, Fresh and hardened properties of self-consolidating fiber-reinforced concrete, ACI Materials Journal 104 (5) (2007) 491–500.
[85] K. Marar, O. Eren, I. Yitmena, Compression specific toughness of normal strength steel fiber reinforced concrete (NSSFRC) and high strength steel fiber reinforced concrete (HSSFRC), Materials Research 14 (2) (2011) 239–247. https://doi.org/10.1590/S1516-14392011005000042
[86] F. Wafa, S. Ashour, Mechanical properties high strength fiber reinforced concrete, ACI Materials Journal 89 (5) (1992) 449–455.
[87] M. Tabatabaeian, A. Khaloo, A. Joshaghani, E. Hajibandeh, Experimental investigation on effects of hybrid fibers on rheological, mechanical, and durability properties of high-strength SCC, Construction and Building Materials 147 (2017) 497–509. https://doi.org/10.1016/j.conbuildmat.2017.04.181
[88] F. Köksal, A. Ilki, M. Tasdemir, Optimum mix design of steel-fibre-reinforced concrete plates, Arabian Journal for Science and Engineering 38 (11) (2013) 2971–2983. https://doi.org/10.1007/s13369-012-0468-y
[89] G. Ruiz, Á. De La Rosa, S. Wolf, E. Poveda, Model for the compressive stress- strain relationship of steel fiber-reinforced concrete for non-linear structural analysis, *Hormigón y Acero* 69-Suppl. 1 (2018) 75–80. https://doi.org/10.1016/j.hya.2018.10.001
[90] G. Ruiz, Á. De La Rosa, E. Poveda, Relationship between residual flexural strength and compression strength in steel-fiber reinforced concrete within the new Eurocode 2 regulatory framework, Theoretical and Applied Fracture Mechanics 103 (2019) 102310. https://doi.org/10.1016/j.tafmec.2019.102310
[91] Á. De La Rosa, G. Ruiz, E. Poveda, Study of the compression behavior of steel-fiber reinforced concrete by means of the response surface methodology, Applied Sciences 9:24 (2019) 5330. https://doi.org/10.3390/app9245330
[92] M. Sargin, Stress-strain Relationship for Concrete and the Analysis of Structural Concrete Sections, Studies series, Solid Mechanics Division, University of Waterloo, 1971.
[93] EN 1994-1-1, Design of Composite Steel and Concrete Structures, European Committee for Standardization–CEN, 2013.
[94] EN 1993-1-1, Design of Steel Structures: General rules and rules for buildings, European Committee for Standardization–CEN, 2005.
[95] G. Hanswille, G. Sedlacek, D. Anderson, The use of steel grades S460 and S420 in composite structures, Tech. rep., ECCS-EUROFER improvements by TC11 to Eurocode 4 (1996).
[96] CEN, Eurocode 4, Design of composite steel and concrete structures. Part 1-1: Part 1-1: General rules and rules for buildings, prEN 1994-1-1: 2022, available through the National members at CEN TC250/SC4 until approved as EN (2022).
[97] M. Schäfer, Q. Zhang, M. Banfi, Background document on materials and limits for plastic moment resistance, Tech. rep., European Mandate M515, CEN/TC250/SC4.T6, CEN-Documents CEN/TC250/SC4 (February 2022).
[98] EN 10025, Hot rolled products of structural steels, European Committee for Standardization–CEN, 2019.
[99] M. Schäfer, Q. Zhang, Zur dehnungsbegrenzten Momententragfhgikeit von Flachdecken in Verbundbauweise – Grenzen der plastischen Bemessung, Stahlbau 88 (7) (2019) 653–664.